HHS Public Access

Author manuscript

Biomaterials. Author manuscript; available in PMC 2022 November 29.

Published in final edited form as:

Biomaterials. 2021 September ; 276: 121019. doi:10.1016/j.biomaterials.2021.121019.

Effects of purified exosome product on rotator cuff tendon-bone healing in vitro and in vivo

Ye Ren[a,b], **Shuwei Zhang**[a], **Yicun Wang**[a], **Daniel S. Jacobson**[a], **Ramona L. Reisdorf**[a], **Tomoyuki Kuroiwa**[a], **Atta Behfar**[c], **Steven L. Moran**[a], **Scott P. Steinmann**[d], **Chunfeng Zhao**[a,*]

[a]Department of Orthopedic Surgery, Mayo Clinic Rochester, Rochester, MN, USA

[b]Department of Orthopedic Surgery, Tongji Hospital, Tongji Medical College, Huazhong University of Science and Technology, Wuhan, Hubei, China

[c]Department of Cardiovascular Medicine, Center for Regenerative Medicine, William J. von Liebig Center for Transplantation and Clinical Regeneration, Mayo Clinic Rochester, MN, USA

[d]Department of Orthopedic Surgery, University of Tennessee Health Science Center College of Medicine, Chattanooga, TN, USA

Abstract

Exosomes have multiple therapeutic targets, but the effects on healing rotator cuff tear (RCT) remain unclear. As a circulating exosome, purified exosome product (PEP) has the potential to lead to biomechanical improvement in RCT. Here, we have established a simple and efficient approach that identifies the function and underlying mechanisms of PEP on cell-cell interaction using a co-culture model in vitro. In the in vivo trial, adult female Sprague-Dawley rats underwent unilateral surgery to transect and repair the supraspinatus tendon to its insertion site with or without PEP. PEP promoted the migration and confluence of osteoblast cells and tenocytes, especially during direct cell-cell contact. Expression of potential genes for RCT in vitro and in vivo models were consistent with biomechanical tests and semiquantitative histologic scores, indicating accelerated strength and healing of the RC in response to PEP. Our observations suggest that circulating exosomes provide an effective option to improve the healing speed of RCT after surgical repair. The regeneration of enthesis following PEP treatment appears to be related to a

*Corresponding author. Department of Orthopedic Surgery, Mayo Clinic, 200 First St SW, Rochester, MN, 55905, USA., zhao.chunfeng@mayo.edu (C. Zhao).

Declaration of competing interest

The authors declare that they have no known competing financial interests or personal relationships that could have appeared to influence the work reported in this paper.

Credit author statement

Ye Ren: Conceptualization, Study Design, Experiment (surgery and outcome measures), Data Collection and Formal analysis, Data Interpretation, Manuscript drafting, Manuscript editing, Manuscript finalizing, Shuwei Zhang: Study Design, Formal analysis, Manuscript drafting, Manuscript editing, Manuscript finalizing, Yicun Wang: Study Design, Formal analysis, Manuscript drafting, Manuscript editing, Manuscript finalizing, Daniel S. Jacobson: Study Design, Formal analysis, Data Interpretation, Manuscript editing, Manuscript finalizing, Ramona L. Reisdorf: Study Design, Formal analysis, Data Interpretation, Manuscript editing, Manuscript finalizing, Tomoyuki Kuroiwa: Study Design, Formal analysis, Manuscript editing, Manuscript finalizing, Atta Behfar: Conceptualization, Study Design, Data Interpretation, Manuscript editing, Manuscript finalizing, Steven L. Moran: Conceptualization, Study Design, Data Interpretation, Manuscript editing, Manuscript finalizing, Scott P. Steinmann: Conceptualization, Study Design, Data Interpretation, Manuscript editing, Manuscript finalizing, Chunfeng Zhao: Conceptualization, Study Design, Formal analysis, Data Interpretation, Manuscript drafting, Manuscript editing, Manuscript finalizing

mutually reinforcing relationship between direct cell-cell contact and PEP activity, suggesting a dual approach to the healing process.

Keywords

Cell communication; Co-culture; Exosome; PEP; Rotator cuff tear

1. Introduction

Rotator cuff tear (RCT) is a common pathologic condition, resulting in pain, disability, expensive treatment, and lost work [1,2]. Surgical repair of RCT is a common and effective treatment [3]; however, the postoperative re-tear rate is high [4]. To improve surgical outcome and reduce tearing postoperatively, studies have focused on biologic and biomechanical factors to enhance tendon-bone healing [5]. Different approaches have been tried, such as using tissue-engineered tendon that combines a scaffold with mechanical properties similar to the native tendon, growth factors that promote cell proliferation and differentiation, and pluripotent stem cells [6–9]. However, due to limitations of cellular and biologic complexities for clinical application, biologic enhancement of RC healing is still an unsolved clinical issue in need of a solution.

Recently, exosomes have attracted attention because of their beneficial roles in cell-cell interaction, signal transduction, and essential cell biologic processes. Exosomes are nanosized bilayer-enclosed extracellular particles that contain numerous nucleic acid molecular constituents such as DNA, mRNA, microRNA, lncRNA, and multiple proteins, which can cross cellular boundaries and affect physiologic and pathologic processes of recipient cells [10,11]. Research shows that tenocytes secrete exosomes, which can initiate the tenogenic differentiation of mesenchymal stem cells (MSCs) in a transforming growth factor-β – dependent manner [12]. Exosomes also can be secreted by bone marrow macrophages, which leads to activation of fibrogenesis in tendon cells [13]. Furthermore, exosomes are now thought to be biologically active and play an important role in healing of the Achilles tendon [14]. It is plausible that multiple stimuli, both mechanical and inflammatory, lead to the development of an exosome-rich microenvironment as an attempt to heal injured tissues or organs [15,16]. Wang et al. [17] have demonstrated that human adipose–derived stem cell exosomes can decrease atrophy and degeneration in torn RC muscles, and even improve muscle biomechanical properties and regeneration. To date, a paucity of literature examines the role of exosomes used in RCT repair and its effect on the tendon-bone healing process.

Purified exosome product (PEP) is manufactured and supplied by the Advanced Product Incubator (API) at the Mayo Clinic Center for Regenerative Medicine, which supports clinical translation of innovative discoveries within our institution. As a current Good Manufacturing Practices (GMP) facility, API adheres to rigorous standards set forth by the US Food and Drug Administration ensuring a high-quality medical-grade product (RION, LLC). PEP production involves separating plasma from blood, isolating a solution of exosomes from separated plasma with filtration and centrifugation, and encapsulating

exosomes according to the patent described (US Patent 20160324A1). It is then formulated and stored as a stabilized lyophilized powder in vials, which allows for storage at room temperature.

As a blood-derived product, PEP may have great potential to stimulate tissue healing and regeneration. In a previous study, we detected the characterization of PEP and observed the effects on tenocyte proliferation ability, migration capability, tendon-related gene expression, total collagen deposition, and cellular apoptosis. It is established that PEP shows superiority in vitro trials [18]. Shi G et al. demonstrated that the 20 % TISSEEL-PEP could promote tendon repair in a canine ex vivo model [19]. Shi A et al. showed 20 % TISSEEL-PEP could enhance ischemic wound healing in vitro and in vivo [20]. In addition, Kisby et al. found that PEP injection was effective for vaginal wound healing in a porcine mesh exposure model. Thus, PEP certainly deserves attention and has great therapeutic potential for repairing damaged tissues [21]. However, the healing influence of PEP on RC repair remains unclear.

This study aimed to 1) investigate the effects of PEP on osteoblasts and tenocytes in a new co-culture model; 2) determine whether PEP treatment improves tendon-bone healing in a rat RCT model; and 3) determine the molecular mechanism by which PEP induces tendon-bone healing. We hypothesize that PEP could upregulate tenocyte healing through promotion of cell proliferation and migration, and that local implantation of PEP could activate certain genes or signal pathways that are critical for enthesis healing.

2. Materials and methods

2.1. Primary cells, culture conditions, and identification

Primary osteoblasts were isolated from the calvaria of neonatal rats that had been euthanized—a process which did not affect the osteoblasts—under Institutional Animal Care and Use Committee (IACUC)-approved guidelines using methods described previously [22]. To harvest osteoblasts, calvaria segments were first immersed in a mixture of 0.1 % (wt/vol) collagenase I and 0.05 % trypsin with 0.004 % ethylenediaminetetraacetic acid for 60 min. Cells were then harvested from the third to fifth immersions and cultured in minimum essential medium α (Invitrogen) supplemented with 10 % fetal bovine serum (Gibco) and 1 % penicillin-streptomycin (Gibco) at 37 °C and 5 % CO_2. To test the osteogenic potential of the primary osteoblasts and PEP, we established 3 groups: The above medium served as the negative control group; the above medium supplemented with PEP served as the positive control group; and the StemPro Osteogenesis Differentiation Kit (A1006601, ThermoFisher, Scientific, Waltham, MA, USA) served as the osteogenic inductive group.

Osteoblasts were identified with alkaline phosphatase (ALP) staining. After being cultured for 7 and 14 days, the primary osteoblasts were washed twice with cold phosphate-buffered saline (PBS), fixed with 4 % paraformaldehyde for 30 min, rinsed with deionized water, and stained with an ALP staining kit (ab242287, Abcam) for 30 min under protection from direct light, according to the manufacturer's instructions. Images were then obtained with a Nikon camera.

Primary tenocytes were isolated from 8-week-old female Sprague-Dawley rats euthanized under IACUC-approved guidelines, using methods described previously [23]. Rat flexor tendons were harvested and the paratendon sheath layer was separated by gentle scraping. Tendons were washed 3 times with sterile PBS, cut into small segments, and cultivated with conditioned medium as described above until confluent growth occurred. The cell culture medium was refreshed every 3 days. Cells from the third to sixth passages were used for all trials. The tenocytes were identified by detection of tendon-specific genes: collagen type 1 (*Col1*), collagen type 3 (*Col3*), and Scleraxis (*SCX*) expression [24]. For quantitative reverse transcriptase–polymerase chain reaction (RT-PCR), the value of each mRNA expression was normalized by glyceraldehyde 3-phosphate dehydrogenase (*GAPDH*) mRNA expression; the rat primary osteoblasts served as the control group.

2.2. Co-culture model

According to the co-culture model shown by Bogdanowicz et al. [25], we created a new simple co-culture model using a 6-well plate and cryopreservation tube. In addition to the osseous, interface, and tenocyte regions, the new model had an additional point of entry for a drug vehicle. Cell culture–grade agarose (Sigma-Aldrich) was poured into the 6-well plate and cut into 3 holes using the cryopreservation tube, leaving a divider of about 3 mm in width. The model was then transferred to a new 6-well plate and fixed with uncoagulated agarose to the bottom of the plate (Fig. 1A–E). The rat primary osteoblasts were seeded on the slightly larger hole to the left, and tenocytes on the slightly larger hole to the right. The small hole was for the PEP vehicle (see below for PEP preparation, Fig. 2B). After allowing 30 min for cell attachment, culture medium was added until the model was nearly submerged. Co-cultures were incubated for 2 days, the divider between 2 kinds of cells was cut, and the drug vehicle was added into the small hole. No drugs were added to the control group. Culture medium overflowed the model and was changed every 3 days. Cell migration into the interface region was recorded twice daily using the IncuCyte HD system (IncuCyte ZOOM, Essen BioScience Inc). The cell boundary was manually traced using Photoshop CS6 (Adobe). For the PCR test, the model was moved and washed with ice-cold PBS at 3 days after direct contact of the 2 cells. Cells were then detached from the plate with cell scrapers in their respective regions and stored with TRIzol (TRI Reagent, Sigma-Aldrich) in tubes, which were stored at −80 °C for the PCR test.

2.3. Animal study design and rat RCT model

Thirty-six Sprague-Dawley rats (adult females, 4–5 months old, 258–552 g) were used. They were randomly divided into 3 groups, and right shoulders were used as the surgical sides (n = 12 for all groups): repair-alone group; operation + TISSEEL (Baxter International) (TISSEEL group); and repair + TISSEEL + PEP (TISSEEL-PEP group). Six weeks after surgery, rats were euthanized via CO_2 asphyxiation (n = 8 for biomechanical testing, and 4 rats for both histologic analysis and PCR test for each group). The left shoulders served as the normal control group (Fig. 3). Rats were anesthetized with 2%–3% isoflurane in 2 L/min 100 % oxygen delivered via mask until disappearance of the toe-pinch reflex via induction chamber. An intramuscular injection of meloxicam (1 mg/kg) was given as preemptive analgesia. Each rat was placed on a warm plate to maintain body temperature and reduce the risk of hypothermia. Anesthesia was maintained with a continuous flow of

1.5%–2% isoflurane in 1 L 100 % oxygen mixture via nose cone. The surgical site was scrubbed with ChloraPrep (BD), and the skin was incised with a sterile #15 scalpel blade in a transverse direction, about 1 cm outside the deltoid muscle. The supraspinatus tendon from the subscapularis tendon anteriorly and the infraspinatus tendon posteriorly were identified and separated. The supraspinatus tendon was then transected at its insertion site on the greater tuberosity. To fresh the insertion site, tendon fibers were scraped at the insertion site with a scalpel. Then, one end of the double-armed 5–0 Ethibond suture (Ethicon Inc) was passed through the tendon transversely, and small loops were made on both sides of the tendon using the modified Mason-Allen suture technique (Fig. 4B, E, and 4F). A 0.5-mm hole was drilled transversely in the anterior-posterior direction through the proximal part of the humerus, and the other end of the suture was passed through the 0.5-mm hole (Fig. 4G). TISSEEL, with or without seeded PEP (depending on the treatment group), was placed on the repair site before tying the suture to the tendon at its insertion point on the greater tuberosity (Fig. 4A, C, and 4D). The detached deltoid muscle was repaired with a 4–0 polyglactin 910 suture (Vicryl, Ethicon Inc), and the skin with a 3–0 polyglactin 910 suture (Vicryl, Ethicon Inc) (Fig. 4H). A water-ibuprofen mixture (15 mg/kg) was administered daily for 1 week postoperatively in all groups. These doses were recommended by a laboratory animal veterinarian and approved in the IACUC protocol.

2.4. Preparation of PEP and fibrin sealant (TISSEEL) with and without PEP

PEP was obtained from the API at the Mayo Clinic Center for Regenerative Medicine. The product was formulated and stored in a stabilized lyophilized powder form in vials to allow for room temperature storage until processing (Fig. 2A).

Fibrin sealant is a biodegradable pulp-like tissue that can be used as a drug delivery vehicle, and is very effective at achieving a local and sustained release of exosomes. Before preparation of the TISSEEL kit (Baxter International), a vial of sealed PEP powder was mixed with 1 mL PBS (Gibco) to prepare the 100 % (vol/vol) PEP solution. We added 400 μL PEP solution into the 600 μL $CaCl_2$ solution (one of the contents of the TISSEEL kit), and the solution was normalized to a 40 % (vol/vol) concentration. Manufacturer directions were then followed to finish kit preparation (Fig. 2B). The final concentration of PEP in TISSEEL was 20 % (vol/vol). The gel was manually cut into small cubes (3 × 3 × 3 mm). In the co-culture model, a single cube was placed into the small hole in one well of a 6-well plate. The culture medium with PEP gel was used to simulate the PEP microenvironment in vivo. For osteogenic induction, the medium with PEP as described above was used as the positive control group. For the in vivo trial, the cube was placed directly on the RC repair site, between the supraspinatus tendon and the greater tuberosity.

2.5. Transmission electron microscopy

Transmission electron microscopy (TEM) observation was performed with a JEOL JEM-1400 Plus 120 kV Transmission Electron Microscope (JEOL Ltd). Before the TEM test, a vial of sealed PEP was mixed with 1 mL PBS (Gibco) to prepare the 100 % (vol/vol) PEP solution. According to the previous publication [26], 50 μL of the PEP solution was transferred to a microcentrifuge tube and 1 mL 2.5 % glutaraldehyde (pH 7.0) in 0.1 M sodium cacodylate solution was added, then mixed for 1 h at 4 °C. Fixed samples were

washed in sodium cacodylate buffer (pH 7.4) 3 times for 10 min each. Next, samples were post-fixed in 2 % osmium tetroxide for 1 h at 4 °C and washed in buffer, dehydrated, and stained with 2 % uranyl acetate according to the standard protocol. PEP (50-μL sample per grid) was examined under a transmission electron microscope at 80 kV and electron micrographs were taken.

2.6. Nanoparticle tracking analysis

Size distribution and concentration of PEP were determined using a nanoparticle tracking characterization system (NanoSight NS300, Malvern Panalytical). The PEP solutions (100 %, vol/vol) were diluted 1000 times with 1 mL PBS diluent before loading into the sample chambers. PEP concentration, mean, and mode PEP size were analyzed using NTA 3.2 analytical software (Malvern Instruments).

2.7. Biomechanical testing of RCT repair

At 6 weeks post treatment, rats were euthanized by carbon dioxide inhalation to evaluate tissue healing. The peritendinous tissue of the supraspinatus tendon and the humerus was then removed completely with surgical loupes. After embedding the humerus in polymethylmethacrylate in a custom-designed fixture and holding the proximal end of the tendon in a spring-loaded clamp custom built for testing, the specimens were subjected to a preload of 0.2 N and pre-conditioned for 5 cycles of 0.1 mm displacement at a rate of 0.1 mm/s, then tested until failure under uniaxial tension at a rate of 0.1 mm/s (Fig. 4I). Finally, ultimate load to failure and stiffness were calculated from the force-displacement curve generated by a custom MATLAB program (MathWorks).

2.8. Histologic analysis

After euthanization at 6 weeks, the repair site at the supraspinatus tendon and its bony insertion was carefully dissected in each group. Specimens were fixed overnight with 10 % formaldehyde and then placed in 14 % ethylenediaminetetraacetic acid. Specimens were placed in 30 %, 50 %, and 70 % ethanol alcohol for at least 30 min each before submission to the core laboratory for paraffin embedding. All specimens were embedded in Tissue-Tek (Sakura) and cut into coronal sections (10 μm thick) with a Leica CM1850 cryostat (Leica Biosystems). Histologic changes were analyzed with hematoxylin-eosin staining, Masson trichrome staining, and Picrosirius red staining. Picrosirius red stained tissue slices were observed by polarized light microscopy (BH2, Olympus).

Based on the literature [27,28], we assessed collagen fiber continuity, parallel orientation, density, vascularity, and cellularity at the tendon-bone interface. Histologic findings were evaluated using a semiquantitative scoring system (0–3 grades per item). For collagen fiber continuity and collagen fibers oriented parallel to each other, scoring was defined by percentage: 0 = 0%–25 % of proportion; 1 = 25%–50 % of proportion; 2 = 50%–75 % of proportion; and 3 = 75%–100 % of proportion. For collagen fiber density, scoring was defined by percentage: 0 = very loose, 1 = loose, 2 = dense, and 3 = very dense. For vascularity and cellularity, scoring was defined by percentage: 0 = absent or minimally present, 1 = mildly present, 2 = moderately present, and 3 = severe or markedly present. Each slide was examined under an Olympus microscope (Olympus) and analyzed

using ImageJ software (National Institutes of Health). Four samples were assessed by 2 independent observers for each group.

2.9. RNA isolation and quantitative PCR

In the in vitro trial, after reaching the measurement time points, cells in corresponding regions (osteoblast region, tenocyte region, and interface region) were washed with PBS and detached by scraping separately. In the in vivo trial, tendon-bone tissues were dissected and flash-frozen in liquid nitrogen, then crushed with an abrasive tool. After homogenization, total RNA was extracted and purified per the manufacturer's instructions using TRIzol Plus RNA Purification Kit (Invitrogen). Total RNA was then quantitated using a NanoDrop 1000 spectrophotometer (Thermo Fisher Scientific) and cDNA synthesis (RT-PCR) was performed by iScript cDNA Synthesis Kit (Bio-Rad Laboratories). Total RNA (1 μg) was reverse transcribed to complementary DNA using the ThermoScript RT kit (Invitrogen). Real-time PCR was performed in triplicate as previously described, and values were normalized using *GAPDH* as the control. For detection of gene marker expression, primers for tenocyte-related gene markers (*Col1*, *Col3*, *SCX*, tenomodulin (*Tnmd*), *EGR1* (early growth response protein 1), decorin (*DCN*)), osteoblast-related gene markers (secreted phosphoprotein 1 (*Spp1*), tenascin C (*TNC*), RUNX family transcription factor 2 (*Runx2*), insulinlike growth factor 1 (IGF-I)), lipid metabolic related gene marker (peroxisome proliferator-activated receptor gamma (*PPARG*)) and chondrogenic related gene markers (*Col2,* cartilage oligomeric matrix protein (*COMP*))were performed.

2.10. Statistical analysis

Data were presented as mean (SD). Each trial was performed independently at least 3 times. Kruskal-Wallis one-way analysis of variance test with Dunn test were used for determining statistical significance for 2-group comparisons and multiple-group comparisons, respectively. Statistical comparisons between 2 groups were analyzed by nonpaired Student *t*-test or Mann-Whitney test. All statistical tests were performed using GraphPad Prism 8 (GraphPad Software Inc). Results with asterisks were considered statistically significant (*$P < .05$, **$P < .01$, ***$P < .001$, ****$P < .0001$).

3. Results

3.1. Results from in vitro experiment

3.1.1. Morphologic characterization of PEP—Consistent with our previous results, TEM results indicate that exosomes of PEP exhibit the typical spherical vesicles with lipid-bilayer–surrounded structure (Fig. 2C). The NanoSight report shows that vesicle sizes of PEP ranged from 56.4 to 151 nm and mean size 96.9 ± 2.8 nm, representing the standard size range of exosomes. PEP solution at 100 % was calculated to be approximately 1.9×10^{11} particles/mL (Fig. 2D).

3.1.2. Identification of rat primary osteoblasts and tenocytes—We selected the calvaria cells isolated from neonatal rats as rat primary osteoblasts. The ALP activity of osteoblasts was gradually increased as the cultivation time prolonged (from day 7 to day 14). In the osteogenic induction media, the osteoblasts showed more osteogenesis and enhanced

further as the culture time was increased. However, the PEP group did not properly show more osteogenic capacity. This result suggests that the 20 % TISSEEL-PEP did not enhance osteoblast activity when compared to control under osteogenic conditions in an vitro co-culture model: there was not an extensive attempt to see if osteoblast activity was dependent on incubation time or the concentration of PEP in the culture (Fig. 1F).

PCR results showed that the relative mRNA expression of tendon-related genes was significantly upregulated compared with the control (osteoblast) group. Furthermore, *SCX* was directly related to tendon development and differentiation, indicating that the identification of the primary cell type corresponds very well to the tendon-origin (Fig. 1G).

3.1.3. Effects of PEP on morphology and outgrowth of the interface region—

Our co-culture model was refined as described in the Methods, with more narrow boundary (≈2–3 mm) between 2 kinds of cells (Fig. 1D). This model allowed us to observe the migration and fusion of the cells within 8 days or fewer. Histologic growth patterns of the osteoblast region, tenocyte region, and interface region were manually pseudocolored at days 0, 2, 4, 6, and 8 using Photoshop CS6 (Adobe Systems) (Fig. 5). Area coverages were manually measured to calculate gap area and fusion area using ImageJ software. The initial gap area of intervention group (PEP group) was 5.17 ± 0.22 mm^2 (n = 6), and 3.37 ± 0.19 mm^2 (n = 6) of the control group (no PEP). Cell growth was significantly increased in all regions following exposure to PEP. Cell migration was more significant in the interface of the PEP group compared to the normal group. In the PEP group, cells had been confluent at day 4, and the fusion area was 0.47 ± 0.14 mm^2 (n = 6) at day 8. However, in the control group, cells began to become confluent at day 6, and the fusion area was only 0.20 ± 0.17 mm^2 (n = 6) at day 8 (Fig. 5).

3.1.4. Changes of mRNA levels—

In the in vitro trial, mRNA levels of Col1, TNC, DCN, SCX, Spp1, and EGR in the PEP group at day 9 significantly increased compared to the PEP group at day 3 in the interface region ($P < .05$). mRNA levels of Col3, TNC, Spp1, EGR, and PPARG in the PEP group at day 6 significantly increased compared to the PEP group at day 3 in the interface region ($P < .05$). Also in the PEP group, co-culture with direct cell-cell contact increased the expression of Col3, TNC, Spp1, PPARG, and EGR compared to co-cultures without direct cell-cell contact (Fig. 6A–G).

3.2. Results from in vivo experiment

3.2.1. Biomechanical testing—

Maximum load of the repair RC at 6 weeks after surgery revealed no statistically significant difference between the TISSEEL-PEP and the normal control group. Maximum tensile load was 22.36 ± 1.51 N (n = 8) in the normal control group and 21.83 ± 1.78 N (n = 8) in the TISSEEL-PEP group. Compared with the other 3 groups, the maximum load of the repair-only group (16.63 ± 0.67 N, n = 8) was the lowest, and significant differences were found between the TISSEEL-PEP group and between the normal control group ($P < .01$). The load in the TISSEEL group (18.62 ± 0.77 N, n = 8; $P = .03$) fell between the repair-only group and the TISSEEL-PEP group and was significantly different from the normal control group (Fig. 4J). Similar results were seen in stiffness for the 4 groups. The TISSEEL-PEP group exhibited a stiffness value of

10.41 ± 4.71 N/mm, which showed similarities to the normal control group (14.06 ± 3.31 N/mm; $P = .11$). Values of stiffness increased gradually for the repair-alone group to the TISSEEL-PEP group and had a significant difference between the repair-alone group (6.12 ± 1.9 N/mm) and the TISSEEL-PEP group. Compared with the other 3 groups, there was a significant difference between the TISSEEL group (7.30 ± 1.58 N/mm; $P = .001$) and the normal control group (Fig. 4K).

3.3. Histologic analysis

In the normal control group, highly aligned collagen fibers were interdigitated into mineralized fibrocartilage passing through the unmineralized fibrocartilage region. After 6 weeks, specimens in the TISSEEL-PEP group demonstrated that the tendon-bone interface had more organized and dense collagen fibers, fewer inflammatory cells, and vascularity, which was similar to the native interface. Besides, an appearance of natural enthesis was also observed in the TISSEEL-PEP group compared with the repair-alone and TISSEEL groups (all $P < .05$) (Table 1; Fig. 7).

In the repair-alone and TISSEEL groups, a mass of inflammatory cells, consisting primarily of polymorphonuclear leukocytes, was present. In addition, a scarlike, looser, and irregular meshwork of collagen fibers was observed in the repair-alone group. The TISSEEL group showed dense inflammatory cells and relatively organized alignment of collagen fibers and scar tissue with newly formed fibrovascular tissues at the tendon-bone interface compared to the repair-alone group ($P < .05$) (Table 1; Fig. 7).

Under polarized microscopy, collage networks appeared to be shorter and thinner in the repair-alone and TISSEEL groups than in the normal control group and TISSEEL-PEP groups. In comparison with the normal control group, collagen in the TISSEEL-PEP group showed relatively promiscuous colors (Fig. 7).

Based on these results, we conclude that PEP with TISSEEL could promote remodeling of collagen fibers and new cartilage-like tissue at the tendon-bone interface after 6 weeks.

3.3.1. Changes of mRNA levels—In the in vivo trial, the TISSEEL-PEP group showed a significant increase in expression of *Col1*, *Col3*, *SCX*, *Tnmd*, *TNC*, *DCN*, and IGF compared to all other groups ($P < .05$) (Fig. 7F). Expressions of osteogenic-related genes (*Spp1*, *Runx2*) and chondrogenic genes (*COMP* and *Col2*) were not detected.

4. Discussion

The response to PEP in the tendon-bone interface was evaluated in this study, and we found that PEP in the treatment of RCT resulted in significant improvement in biomechanical characteristics. Histologic observation revealed well-organized collagen fiber, along with upregulated expression of tendon and tendon-bone–relative markers.

Using MSCs to enhance RC repair has been well studied [29]. With the increasing number of studies in basic and clinical research of RCT repair, the efficacy of MSC therapy has been established. MSCs are progenitors of osteoblasts, chondrocytes, and tenocytes, which

promote differentiation and growth of progenitor cells, collagen remodeling and maturity, osteogenesis, and enrichment of extracellular matrix. MSC-derived exosomes have functions similar to MSCs, which present a promising therapeutic approach for RC regeneration [29]. Via small biological molecules, exosomes act as carriers regulating biological functions locally or by circulation. In addition, exosomes inherently have less immunogenicity than live stem cell transplants, which makes exosomes promising in the fields of regenerative application. Because the structure of the RC is complicated, the process of RC healing is complicated by multiple variables. Exosomes, derived from MSCs, express a variety of angiogenic and angiostatic factors, including human growth factor, insulinlike growth factor binding proteins 2, 3, and 6 (IGFBP2, IGFBP3, and IGFBP6), and others [30]. One study showed that MSC exosomes effectively stimulate the proliferation and osteogenic differentiation of bone marrow stem cells and bone regeneration in a rat model [31]. Another study found that sustained secretion of tenocyte-derived exosomes can induce differentiation of MSCs in a transforming growth factor-β–dependent manner [12]. In a rat model, exosomes derived from human synovial MSCs could prevent osteoarthritis of the knee by enhancing cartilage tissue regeneration [32]. The diversity of ingredients in exosomes leads to the multipotency of exosomes. Thus, we believe that exosomes can accelerate the healing process in RCT by acting on multiple targets and multiple pathways.

Circulating exosomes—those that are released in blood circulation and reflect biological characteristics of living organisms—can arrive in distant tissue and transmit exosomal material to recipient cells for biological function. Proteomic and bioinformatic analyses of maternal circulation exosomes have shown proteins associated with the prepartum processes [33]. Emanueli et al. [34] found that circulating exosomes containing cardiac microRNAs were released after heart surgery. In rheumatoid arthritis patients, circulating exosomes were related to the development of rheumatoid arthritis by adjusting the circulating regulatory T cells [35]. PEP used in our study comes from expired human donor plasma, is relatively easy to access, and is cost-effective compared to other biologic agents. Given PEP's origin and the blood donation policy in the US, we believe that PEP may represent a physiologic state of healthy adults younger than 65 years. PEP is considered an indicator of healthy characteristics, while not causing overexpression of a specific molecule related to a pathologic process. Previous reports have shown that PEP can promote tenocyte proliferation at certain concentrations [18]. To our knowledge, our study is the first to use a human circulating exosome product for RCT healing in a rat model.

As fibrin sealants, TISSEEL (Baxter Healthcare) contains human fibrinogen and thrombin. TISSEEL is a medical adhesive widely used for hemostasis in surgery, and shows good drug encapsulation capabilities for different kinds of drugs (eg, growth factors, synthetic drugs, genes) [36]. In the previous published ex vivo results [19], 20 % TISSEEL-PEP could stably release the extracellular vesicle at least two weeks. Therefore, we used TISSEEL as a vehicle to deliver PEP. Falanga et al. [37] used TISSEEL to deliver MSCs, which accelerated cutaneous wound healing in murine animals and humans. Ivica et al. [38] found that a combination of exosomes and TISSEEL could induce cell migration substantially more than either method on its own. In a murine model of incisional hernia, exosomes combined with fibrin glue had a beneficial effect on anti-inflammation and remodeling [39]. In our study, tendons that were coated with TISSEEL, even without PEP, demonstrated

improved vascularization and cellularity. The use of TISSEEL as a PEP delivery vehicle promoted RCT healing speed and showed no immune rejection reactions over 6 weeks post-surgery. We here first showed that the local delivery of PEP could enhance RC tendon-bone healing. We think the sustained release of PEP to the repair site in the TISSEEL may help regeneration of a fibro-cartilaginous transitional region during healing, leading to improved mechanical characteristics at the RC enthesis. The combined application of TISSEEL and PEP has the following other advantages: 1) Our PEP is manufactured with GMP-grade materials, and TISSEEL is an FDA-approved product that has been used in clinical scenarios; therefore, this cell-free bioactive material can be rapidly translated to clinical application. 2) PEP isolated from expired blood product is cost-efficient. 3) Since exosomes in the PEP were already present in the blood product, there is no need to culture and manipulate specific cells to produce exosomes, which makes the clinical translation more feasible and economic with few hurdles.

Although rats generally have a potent tissue healing ability, study has indicated that the process of RCT repair and regeneration may take up to 8 weeks or more [40]. In our study, biomechanical properties in the TISSEEL-PEP group represent a clear advantage. Comparing the 6-week data with the literature, we show that the strength of TISSEEL-PEP is close to normal RC strength. The histologic results show more organized and tighter collagenous tissue at the tendon-bone interface in the TISSEEL-PEP group. Although close to the normal control group, the TISSEEL-PEP group also shows typical cartilage layers in the RC structure compared to the other groups. We think that it should be fibrocartilage at the healing enthesis. The reasons are as follows: 1. The native enthesis usually consist of tendon, bone and fibrocartilage, not hyaline cartilage. 2. Typically, a repair tissue such as bone or tendon often forms fibrocartilage rather than hyaline cartilage, which quite difficult to regenerate [41]. 3. *Col2* is the dominant collagen type that represents the hyaline cartilage. However, we did not detect any expression of *Col2*, both in vivo and in vitro. In line with our study, Nakagawa et al. [40] report that only retention of fibrocartilage in enthesis could enhance regeneration of bone marrow–derived chondrogenic cells at 8 weeks after RC operation. Moreover, we did not detect expression of gene markers for chondrocytes in the interface region of the co-culture model in vitro, which led us to believe that the regeneration of cartilage must require the combined actions of MSCs and chondrocytes during RCT repair.

Further, the results of gene expression were confirmed through the biomechanical and histologic results. In addition to enhancing IGF expression, PEP was found to promote the upregulation of tendon-related genes (*Col1*, *Col3*, *SCX*, *Tnmd*, and *DCN*), leading to rearrangement of collagen and matrix constituent of the extracellular matrix during RC tendon healing. We reason that PEP plays an important role in releasing pivotal ingredients that help remold the RC structure. In the in vitro co-culture study, osteoblasts and tenocytes were the main cells involved in the RC healing process. PEP could promote the above cells' migration and fusion in vitro culture. We found that PEP showed mild, but not significant, suppression of some genes (*Col3*, *PPARG*, *TNC*, *SPP1*, and *EGR*) at 3 days when cells were in all regions of the co-culture model. However, this trend was almost reversed at 6 and 9 days in osteoblast and tenocyte regions, respectively, without direct cell-cell contact. Interestingly, PEP could promote some genes' expression more substantially (*Col1*, *Col3*,

PPARG, *TNC*, *SPP1*, *DCN*, and *EGR*) at the last 2 time points in the direct cell-cell contact environment. *PPARG* is a gene associated with adipocyte differentiation. A study by Kheirollahi et al. has shown that *PPARG* and *Col1* mRNA levels present a negative correlation in primary human lung fibroblasts, which could explain the similar result seen in our study [42]. In brief, we found that 1) PEP had a lagged timeframe of action at a very early time, and 2) PEP and direct cell-cell contact were interlinked and reinforced each other in vitro, which may explain why the enthesis area of RC had a higher recovery in vivo.

There are some limitations to this study. First, the new culture model was constructed based on the classic 2D culture system, and had the same limitation of lacking long-term maintenance and 3D environment. Second, the new co-culture model included only 2 kinds of cells in enthesis; as a result, we were unable to observe chondrogenic progenitor cells, MSCs, and tendon stem cells, which have differentiation potentials. Third, we used 4- and 5-month-old rats, which correlates with a human age of about 18; therefore, this model represents acute RC injury in young adults. However, since RCT is an age-related problem, future studies in chronic or massive RCT models with older rats should be conducted. Fourth, it unclear if PEP effectiveness would be sex-dependent. Female rats were chosen for the present study because the male rats are more aggressive especially after the operation, which may lead to increasing the risk of unwanted injuries. To minimize the animal usage (sample size), we omitted sexual variables. Fifth, lack of long-time follow-up data and lack of long-time tracking data of TISSEEL-PEP. In an ex vivo experiment reported by Shi G et al. [19], 20 % TISSEEL-PEP could stably release the extracellular vesicle at least two weeks. An in vivo wound healing model by Shi A et al. showed that TISSEEL-PEP could promote ischemic wound healing at least 4 weeks in vivo [20]. To more fully understand the mechanisms of action in the treatment of RCT, future studies should include long-term follow-up and functional analyses.

5. Conclusion

Here we present a novel and clinically translatable bioactive material combined with our GMP-grade PEP and TISSEEL for RC repair and regeneration. The results support our hypothesis that the combination of PEP and TISSEEL improve RC healing. We also used a co-culture in vitro model to reveal the mechanism that demonstrates that PEP increases cell proliferation and migration mainly by upregulating tenogenic markers. We are hopeful that PEP will propel future discoveries leading to improved therapies of RCT.

Acknowledgments

This work was supported and funded by NIH/NIAMS (AR57745) and an Orthopedic Research Review Committee grant from the Department of Orthopedic Surgery, Mayo Clinic.

The authors, their immediate families, and any research foundations with which they are affiliated have not received any financial payments or other benefits from any commercial entity related to the subject of this article.

References

[1]. Khor WS, Langer MF, Wong R, Zhou R, Peck F, Wong JK, Improving outcomes in tendon repair: a critical look at the evidence for flexor tendon repair and rehabilitation, Plast. Reconstr. Surg. 138 (2016) 1045e, 58e.

[2]. Snedeker JG, Foolen J, Tendon injury and repair - a perspective on the basic mechanisms of tendon disease and future clinical therapy, Acta Biomater. 63 (2017) 18–36. [PubMed: 28867648]

[3]. Depres-Tremblay G, Chevrier A, Snow M, Hurtig MB, Rodeo S, Buschmann MD, Rotator cuff repair: a review of surgical techniques, animal models, and new technologies under development, J. Shoulder Elbow Surg. 25 (2016) 2078–2085. [PubMed: 27554609]

[4]. Randelli P, Spennacchio P, Ragone V, Arrigoni P, Casella A, Cabitza P, Complications associated with arthroscopic rotator cuff repair: a literature review, Musculoskeletal surgery 96 (2012) 9–16. [PubMed: 22205384]

[5]. Patel S, Gualtieri AP, Lu HH, Levine WN, Advances in biologic augmentation for rotator cuff repair, Ann. N. Y. Acad. Sci. 1383 (2016) 97–114. [PubMed: 27750374]

[6]. Shahab-Osterloh S, Witte F, Hoffmann A, Winkel A, Laggies S, Neumann B, et al. , Mesenchymal stem cell-dependent formation of heterotopic tendon-bone insertions (osteotendinous junctions), Stem Cell. 28 (2010) 1590–1601.

[7]. Shimomura K, Moriguchi Y, Murawski CD, Yoshikawa H, Nakamura N, Osteochondral tissue engineering with biphasic scaffold: current strategies and techniques. Tissue engineering Part B, Review 20 (2014) 468–476.

[8]. Zhang J, Wang JH, Mechanobiological response of tendon stem cells: implications of tendon homeostasis and pathogenesis of tendinopathy, J. Orthop. Res. : official publication of the Orthopaedic Research Society 28 (2010) 639–643.

[9]. Lejard V, Blais F, Guerquin MJ, Bonnet A, Bonnin MA, Havis E, et al. , EGR1 and EGR2 involvement in vertebrate tendon differentiation, J. Biol. Chem. 286 (2011) 5855–5867. [PubMed: 21173153]

[10]. Isola AL, Chen S, Exosomes: the messengers of Health and disease, Curr. Neuropharmacol. 15 (2017) 157–165. [PubMed: 27568544]

[11]. Valadi H, Ekstrom K, Bossios A, Sjostrand M, Lee JJ, Lotvall JO, Exosome-mediated transfer of mRNAs and microRNAs is a novel mechanism of genetic exchange between cells, Nat. Cell Biol. 9 (2007) 654–659. [PubMed: 17486113]

[12]. Xu T, Xu M, Bai J, Lin J, Yu B, Liu Y, et al. , Tenocyte-derived exosomes induce the tenogenic differentiation of mesenchymal stem cells through TGF-beta, Cytotechnology 71 (2019) 57–65. [PubMed: 30599073]

[13]. Cui H, He Y, Chen S, Zhang D, Yu Y, Fan C, Macrophage-derived miRNA-containing exosomes induce peritendinous fibrosis after tendon injury through the miR-21–5p/smad7 pathway, Mol. Ther. Nucleic Acids 14 (2019) 114–130. [PubMed: 30594070]

[14]. Chamberlain CS, Clements AEB, Kink JA, Choi U, Baer GS, Halanski MA, et al. , Extracellular vesicle-educated macrophages promote early Achilles tendon healing, Stem Cell. 37 (2019) 652–662.

[15]. Masyuk AI, Masyuk TV, Larusso NF, Exosomes in the pathogenesis, diagnostics and therapeutics of liver diseases, J. Hepatol. 59 (2013) 621–625. [PubMed: 23557871]

[16]. Zhang ZG, Buller B, Chopp M, Exosomes - beyond stem cells for restorative therapy in stroke and neurological injury, Nat. Rev. Neurol. 15 (2019) 193–203. [PubMed: 30700824]

[17]. Wang C, Song W, Chen B, Liu X, He Y, Exosomes isolated from adipose-derived stem cells: a new cell-free approach to prevent the muscle degeneration associated with torn rotator cuffs, Am. J. Sports Med. 47 (2019) 3247–3255. [PubMed: 31560856]

[18]. Qi J, Liu Q, Reisdorf RL, Boroumand S, Behfar A, Moran SL, et al. , Characterization of a purified exosome product and its effects on canine flexor tenocyte biology, J. Orthop. Res. : official publication of the Orthopaedic Research Society 38 (2020) 1845–1855.

[19]. Shi G, Wang Y, Wang Z, Thoreson AR, Jacobson DS, Amadio PC, et al. , A novel engineered purified exosome product patch for tendon healing: an explant in an ex vivo model, J. Orthop. Res. : official publication of the Orthopaedic Research Society (2020).

[20]. Shi A, Li J, Qiu X, Sabbah M, Boroumand S, Huang TC, et al. , TGF-beta loaded exosome enhances ischemic wound healing in vitro and in vivo, Theranostics 11 (2021) 6616–6631. [PubMed: 33995680]

[21]. Kisby CK, Shadrin IY, Peng LT, Stalboerger PG, Trabuco EC, Behfar A, et al. , Impact of repeat dosing and mesh exposure chronicity on exosome-induced vaginal tissue regeneration in a porcine mesh exposure model, Female Pelvic Med. Reconstr. Surg. 27 (2021) 195–201.

[22]. Liu B, Lu Y, Wang Y, Ge L, Zhai N, Han J, A protocol for isolation and identification and comparative characterization of primary osteoblasts from mouse and rat calvaria, Cell Tissue Bank. 20 (2019) 173–182. [PubMed: 30887273]

[23]. Zhang J, Wang JH, Characterization of differential properties of rabbit tendon stem cells and tenocytes, BMC Muscoskel. Disord. 11 (2010) 10.

[24]. Jo CH, Lim HJ, Yoon KS, Characterization of tendon-specific markers in various human tissues, tenocytes and mesenchymal stem cells, Tissue engineering and regenerative medicine 16 (2019) 151–159. [PubMed: 30989042]

[25]. Bogdanowicz DR, Lu HH, Multifunction co-culture model for evaluating cell-cell interactions, Methods Mol. Biol. 1202 (2014) 29–36. [PubMed: 24504928]

[26]. Jung MK, Mun JY, Sample preparation and imaging of exosomes by transmission electron microscopy, JoVE : JoVE (2018).

[27]. Yoon JP, Chung SW, Jung JW, Lee YS, Kim KI, Park GY, et al. , Is a local administration of parathyroid hormone effective to tendon-to-bone healing in a rat rotator cuff repair model? J. Orthop. Res. : official publication of the Orthopaedic Research Society 38 (2020) 82–91.

[28]. Chung SW, Song BW, Kim YH, Park KU, Oh JH, Effect of platelet-rich plasma and porcine dermal collagen graft augmentation for rotator cuff healing in a rabbit model, Am. J. Sports Med. 41 (2013) 2909–2918. [PubMed: 24047553]

[29]. Connor DE, Paulus JA, Dabestani PJ, Thankam FK, Dilisio MF, Gross RM, et al. , Therapeutic potential of exosomes in rotator cuff tendon healing, J. Bone Miner. Metabol. 37 (2019) 759–767.

[30]. Hernigou P, Flouzat Lachaniette CH, Delambre J, Zilber S, Duffiet P, Chevallier N, et al. , Biologic augmentation of rotator cuff repair with mesenchymal stem cells during arthroscopy improves healing and prevents further tears: a case-controlled study, Int. Orthop. 38 (2014) 1811–1818. [PubMed: 24913770]

[31]. Qi X, Zhang J, Yuan H, Xu Z, Li Q, Niu X, et al. , Exosomes secreted by human-induced pluripotent stem cell-derived mesenchymal stem cells repair critical-sized bone defects through enhanced angiogenesis and osteogenesis in osteoporotic rats, Int. J. Biol. Sci. 12 (2016) 836–849. [PubMed: 27313497]

[32]. Tao SC, Yuan T, Zhang YL, Yin WJ, Guo SC, Zhang CQ, Exosomes derived from miR-140-5p-overexpressing human synovial mesenchymal stem cells enhance cartilage tissue regeneration and prevent osteoarthritis of the knee in a rat model, Theranostics 7 (2017) 180–195. [PubMed: 28042326]

[33]. Sheller-Miller S, Trivedi J, Yellon SM, Menon R, Exosomes cause preterm birth in mice: evidence for paracrine signaling in pregnancy, Sci. Rep. 9 (2019) 608. [PubMed: 30679631]

[34]. Emanueli C, Shearn AI, Laftah A, Fiorentino F, Reeves BC, Beltrami C, et al. , Coronary artery-bypass-graft surgery increases the plasma concentration of exosomes carrying a cargo of cardiac MicroRNAs: an example of exosome trafficking out of the human heart with potential for cardiac biomarker discovery, PloS One 11 (2016), e0154274. [PubMed: 27128471]

[35]. Wang L, Wang C, Jia X, Yu J, Circulating exosomal miR-17 inhibits the induction of regulatory T cells via suppressing TGFBR II expression in rheumatoid arthritis, Cell. Physiol. Biochem. : int. j. exp.cell. physiol. biochem, and pharmacol 50 (2018) 1754–1763.

[36]. Spicer PP, Mikos AG, Fibrin glue as a drug delivery system, J. Contr. Release : official journal of the Controlled Release Society 148 (2010) 49–55.

[37]. Falanga V, Iwamoto S, Chartier M, Yufit T, Butmarc J, Kouttab N, et al. , Autologous bone marrow-derived cultured mesenchymal stem cells delivered in a fibrin spray accelerate healing in murine and human cutaneous wounds, Tissue Eng. 13 (2007) 1299–1312. [PubMed: 17518741]

[38]. Ivica A, Ghayor C, Zehnder M, Valdec S, Weber FE, Pulp-derived exosomes in a fibrin-based regenerative root filling material, J. Clin. Med. 9 (2020).

[39]. Blazquez R, Sanchez-Margallo FM, Alvarez V, Uson A, Marinaro F, Casado JG, Fibrin glue mesh fixation combined with mesenchymal stem cells or exosomes modulates the inflammatory

reaction in a murine model of incisional hernia, Acta Biomater. 71 (2018) 318–329. [PubMed: 29462710]

[40]. Nakagawa H, Morihara T, Fujiwara H, Kabuto Y, Sukenari T, Kida Y, et al. , Effect of footprint preparation on tendon-to-bone healing: a histologic and biomechanical study in a rat rotator cuff repair model, Arthroscopy : the journal of arthroscopic & related surgery : official publication of the Arthroscopy Association of North America and the International Arthroscopy Association 33 (2017) 1482–1492. [PubMed: 28606577]

[41]. Armiento AR, Alini M, Stoddart MJ, Articular fibrocartilage - why does hyaline cartilage fail to repair? Adv. Drug Deliv. Rev. 146 (2019) 289–305. [PubMed: 30605736]

[42]. Kheirollahi V, Wasnick RM, Biasin V, Vazquez-Armendariz AI, Chu X, Moiseenko A, et al. , Metformin induces lipogenic differentiation in myofibroblasts to reverse lung fibrosis, Nat. Commun. 10 (2019) 2987. [PubMed: 31278260]

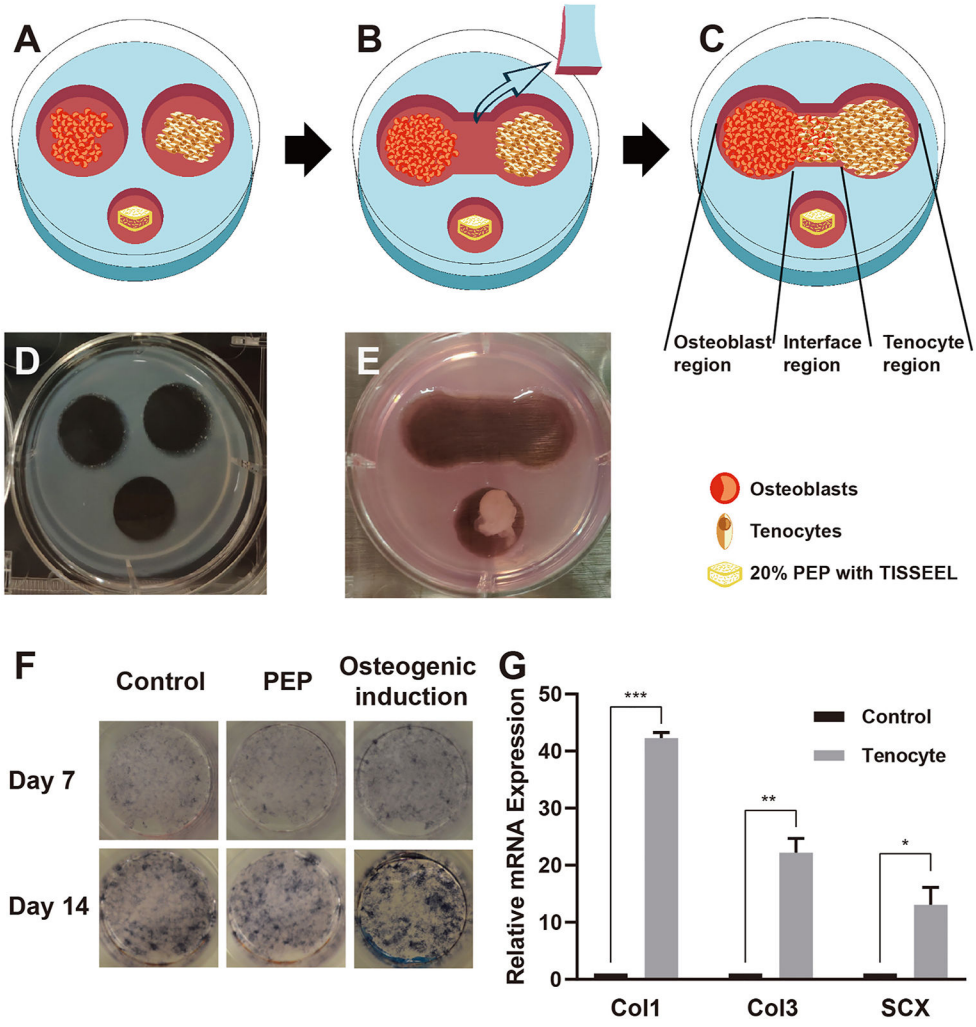

Fig. 1. Co-culture model and cell identification.

A, Schematic representation of the co-culture model, composed of osteoblasts, tenocytes, and PEP gel cube. B, The boundary was cut and moved when cells reached the boundary. C, Schematic representation of the osteoblast region, tenocyte region, and interface region in the co-culture model. D, Photograph of the co-culture model before and, E, after the boundary moved. F, Alkaline phosphatase staining after application of normal culture medium, with PEP or osteogenic induction conditions, day 7 and day 14. G, Relative mRNA expression levels of *Col1*, *Col3*, and *SCX* in primary tenocytes (osteoblasts as the control group). ALP indicates alkaline phosphatase; PEP, purified exosome product; *, $P < .1$; **, $P < .01$; ***, $P < .001$.

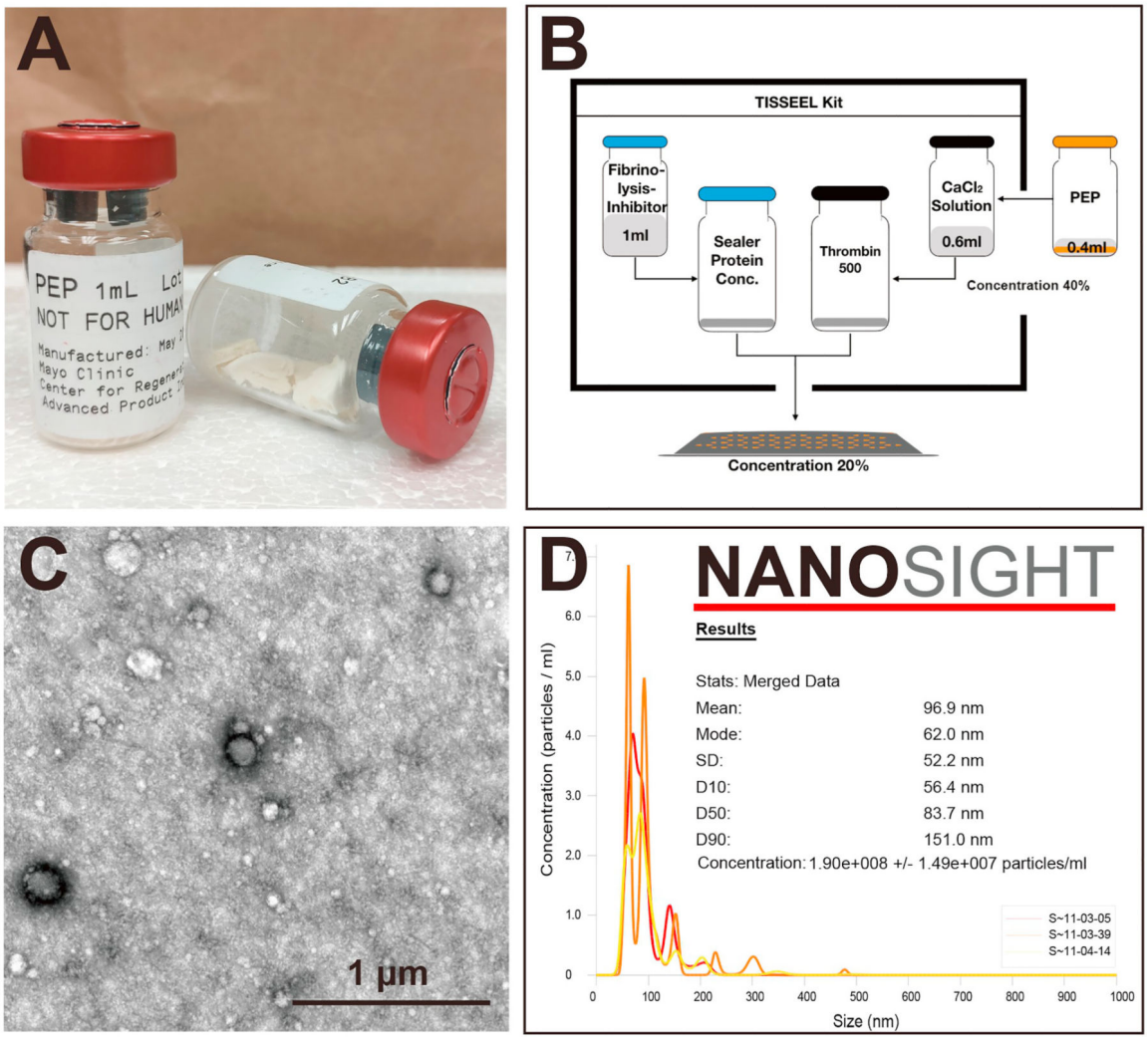

Fig. 2. Morphologic characterization of PEP.

A, PEP was formulated and stored in a stabilized lyophilized powder form in vials to allow for room temperature storage. B, Preparation of fibrin sealant (TISSEEL) with and without PEP. A vial of sealed PEP powder was mixed with 1 mL PBS to prepare the 100 % (vol/vol) PEP solution. PEP solution (400 μL) was added to the 600-μL $CaCl_2$ solution, and the solution was normalized to a 40 % (vol/vol) concentration. Manufacturer directions were then used to finish kit preparation. The final concentration of PEP in TISSEEL was 20 % (vol/vol). C, PEP exhibits the typical spherical vesicles with a lipid-bilayer–surrounded structure. D, The NanoSight report states that vesicle size of PEP ranged from 56.4 to 151 nm and the mean size was 96.9 ± 2.8 nm, representing the standard size range of exosomes. The 100 % PEP solution was calculated to be approximately equal to 1.9×10^{11} particles/mL. PBS indicates phosphate-buffered saline; PEP, purified exosome product.

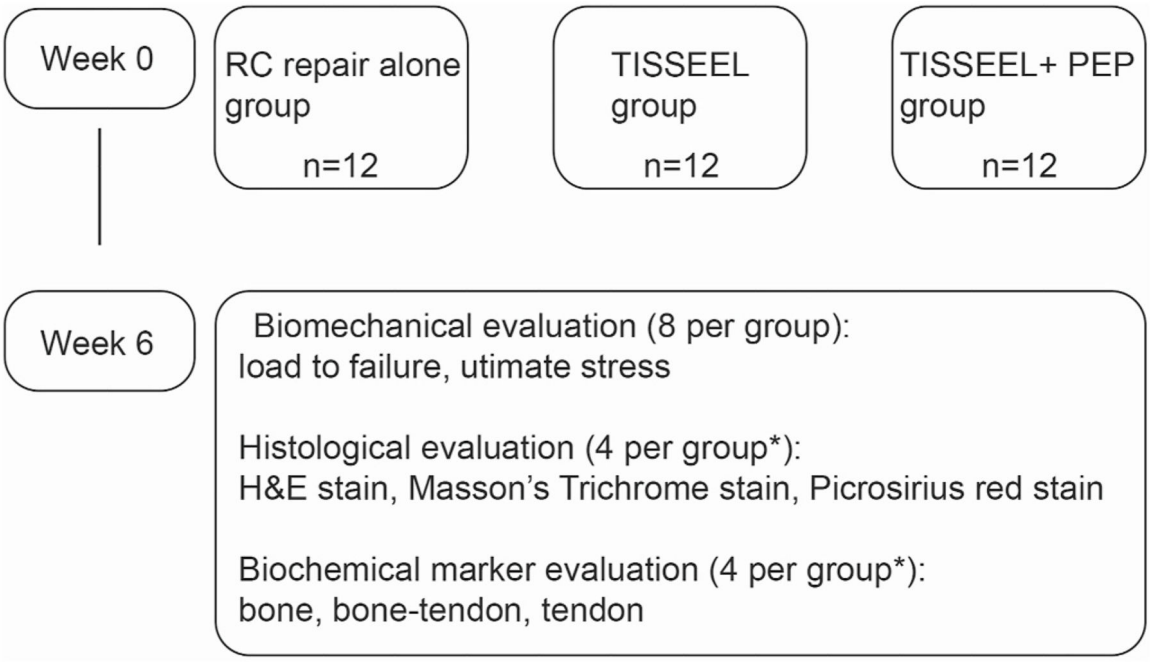

Fig. 3. Flowchart showing the experimental design in the in vivo model.

H&E indicates hematoxylin-eosin; PEP, purified exosome product; RC, rotator cuff; *, the same rats were used in each evaluation.

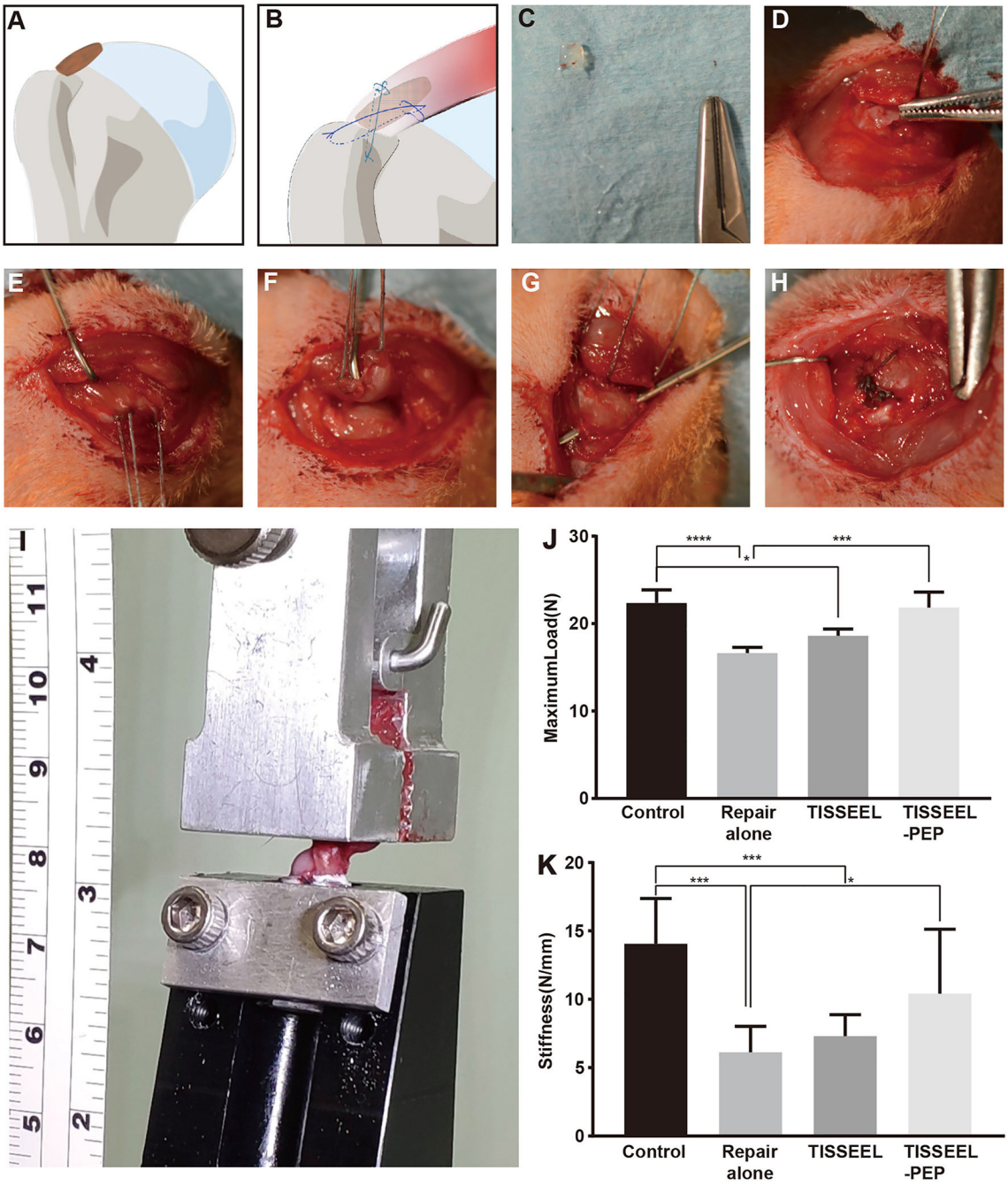

Fig. 4. Surgical procedure and biomechanical testing of RC repair.

A, Local PEP placement at insertion site of the supraspinatus tendon. B, Modified Mason-Allen suture way. C, Gross observation of PEP gel cube before implantation in vivo. D, PEP placed before suturing. E, Two double-armed 5–0 Ethibond sutures were passed through the tendon transversely, and small loops were made on both sides of the tendon. F, The supraspinatus tendon was transected at its insertion site on the greater tuberosity. G, Suture was passed through a 0.5-mm hole drilled transversely at the proximal part of the humerus. H, Gross observation after careful suturing. I, The biomechanical testing system shows the

humerus embedded within a tube of polymethylmethacrylate. The supraspinatus tendon is fixed to the attachment through a clamp at ultimate load to failure. J and K, Results are shown as mean (SD) (n = 8 for each group). The ultimate load to failure and stiffness at 6 weeks were significantly higher after augmentation with PEP compared to the repair-only group. PEP indicates purified exosome product; RC, rotator cuff; *, $P < .1$; ***, $P < .001$; ****, $P < .0001$.

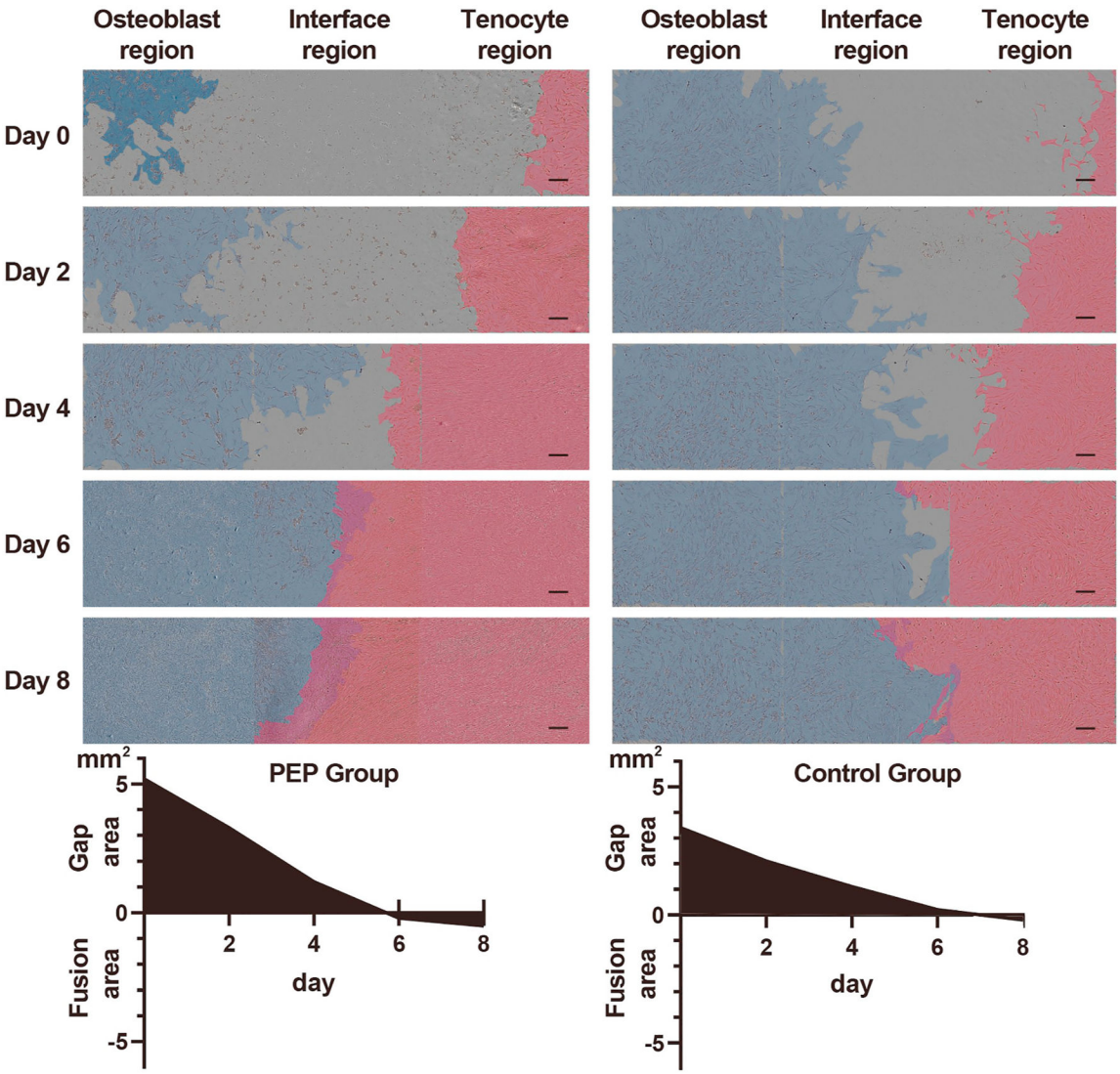

Fig. 5. Cell growth and migration in all regions following exposure to PEP.

Blue indicates the region of osteoblasts, and red indicates the region of tenocytes at various time points (0, 2, 4, 6, and 8 days, n = 6). Left, PEP group. Right, control group (scale bars, 200 μm). Histograms show quantified results of the gap area and the fusion area. PEP indicates purified exosome product.

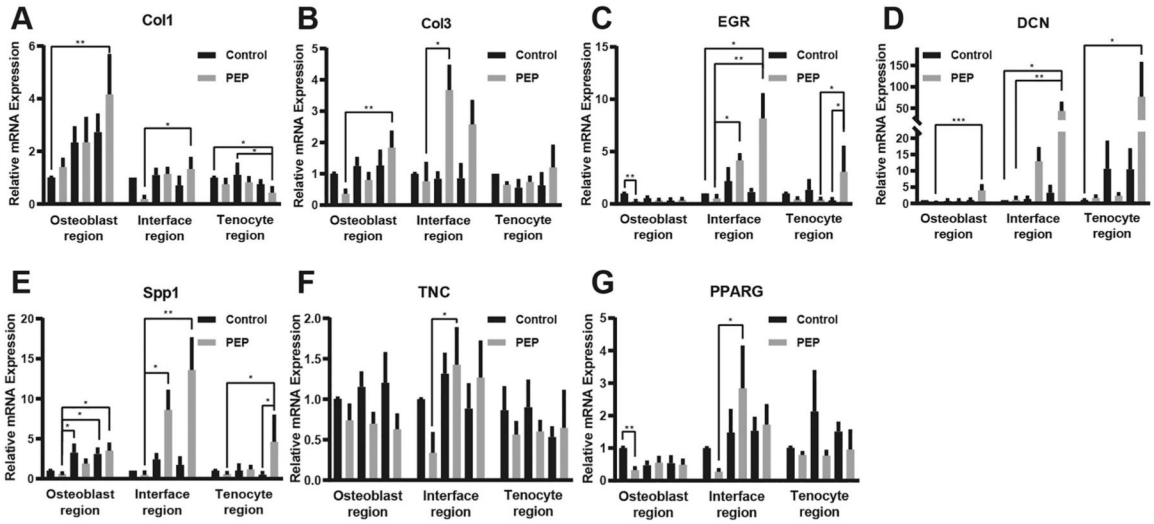

Fig. 6. Result of quantitative RT-PCR verification in the in vitro trial.

A-G, Real-time PCR results of *Col1*, *Col3*, *DCN*, *TNC*, *Spp1*, *EGR*, and *PPARG*-relative mRNA expression 3 days after direct contact of the 2 cells in the in vitro trial. RT-PCR indicates reverse transcription–polymerase chain reaction; *, $P < .1$; **, $P < .01$; ***, $P < .001$.

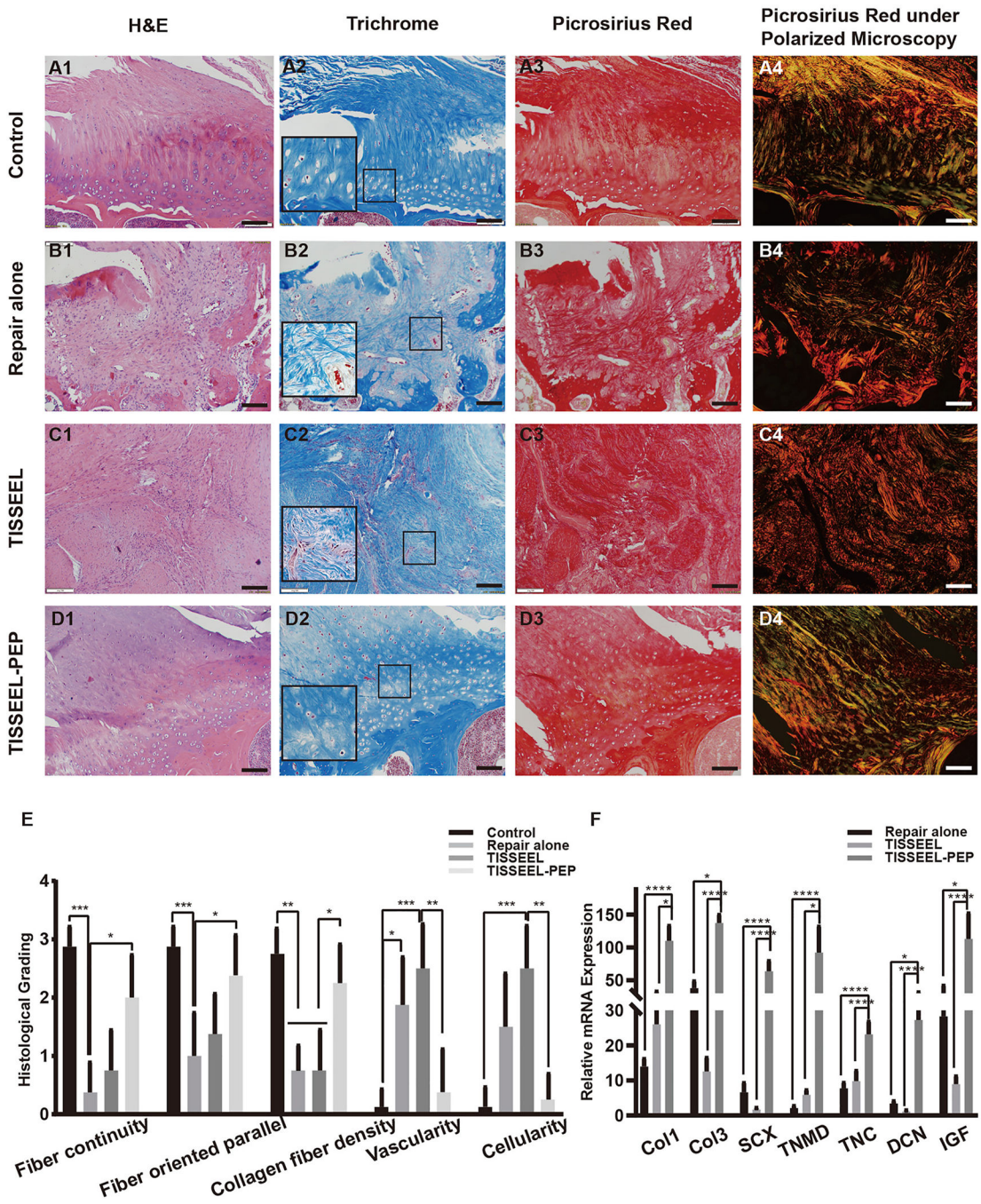

Fig. 7. Histologic analysis and result of quantitative RT-PCR verification in the in vivo trial.
Histology of rat RC tendon and its insertion into the humerus after 6 weeks (Ã E). A, Normal control group. B, Repair-alone group. C, TISSEEL group. D, TISSEEL-PEP group. (A1-D1, H &E staining, × 10; A2-D2, Masson trichrome staining, × 10, black frame, × 20; A3-D3, Picrosirius red stain, × 10; A4-D4, Picrosirius red stain under a polarizing microscope; scale = 100 μM) E, Histologic findings were evaluated using a semiquantitative scoring system. F, Real-time PCR results of *Col1*-, *Col3*-, *SCX*-, *Tnmd*-, *TNC*-, *DCN*-, *Spp1*-, and *IGF-I*–relative mRNA expression after 6 weeks in the in vivo trial. H&E

indicates hematoxylin-eosin; PEP, purified exosome product; RC, rotator cuff; RT-PCR indicates reverse transcription–polymerase chain reaction; *, $P < .1$; **, $P < .01$; ***, $P < .001$; ****, $P < .0001$.

Table 1

Histologic grading of the tendon-bone insertion site after 6 Weeks.

Parameter	Control group (n = 8)				Repair-alone (n = 8)				TISSEEL (n = 8)				TISSEEL-PEP (n = 8)				
	0	1	2	3	0	1	2	3	0	1	2	3	0	1	2	3	*P* Value
Collagen fiber continuity	0	0	1	7	5	3	0	0	3	4	1	0	0	2	4	2	<.0001
Collagen fiber oriented parallel	0	0	1	7	2	4	2	0	1	3	4	0	0	1	3	4	= .0002
Collagen fiber density	0	0	2	6	2	6	0	0	3	4	1	0	0	1	4	3	<.0001
Vascularity	7	1	0	0	0	3	3	2	0	1	2	5	6	1	1	0	<.0001
Cellularity	7	1	0	0	1	3	3	1	0	1	2	5	6	2	0	0	<.0001

Histological findings were evaluated using a semiquantitative scoring system (0–3 grades per item). For collagen fiber continuity and collagen fibers oriented parallel, scoring was defined by percentage as: 0 = 0%–25 % of proportion; 1 = 25%–50 % of proportion; 2 = 50%–75 % of proportion; and 3, = 75%–100 % of proportion. For collagen fiber density, scoring was defined by percentage as: 0 = very loose; 1 = loose; 2 = dense; and 3 = very dense. For vascularity and cellularity, scoring was defined by percentage as: 0 = absent or minimally present; 1 = mildly present; 2 = moderately present; and 3 = severe or markedly present. Four samples were assessed by 2 independent observers (n = 8). Statistical significance of intergroup differences was assessed using Kruskal-Wallis test.